Supporting Information

Searching for cheaper catalysts with high activity and stability in Ce-M-O systems (M=Fe, Co, Ni)

*Ying Zuo, Liping Li, Xinsong Huang and Guangshe Li**

†State Key Lab of Structural Chemistry, Fujian Institute of Research on the Structure of Matter, Chinese Academy of Sciences, Fuzhou 350002, P.R. China.

E-mail: guangshe@fjirsm.ac.cn; Fax: +86-591-83702122

Sample characterization

Part 1. Relevant data and descriptions about synthesis and solubility limit of $Ce_{1-x}M_xO_2$ systems (M=Fe, Co, Ni)

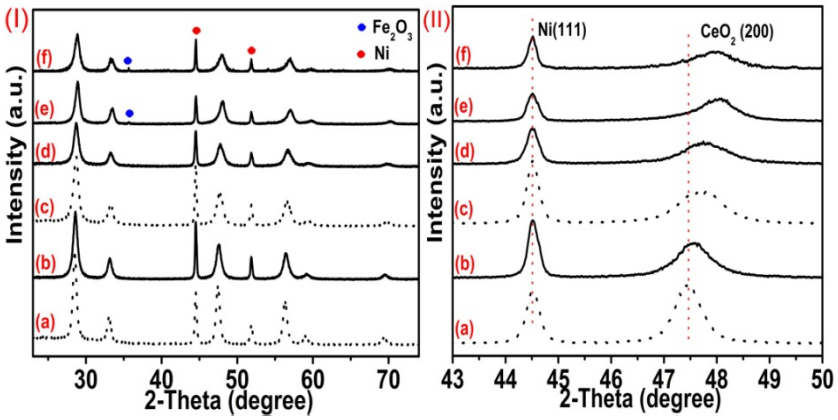

Fig. S1 (I) XRD and (II) amplified XRD patterns of $Ce_{1-x}Fe_xO_2$ system at (a) x=0, (c) 0.10 redraw from literature[1], (b) x=0.05, (d) x=0.15 and (e) x=0.20, and (f) x=0.25.

As shown in Fig. S1 (I), all peaks could be assigned to CeO_2 (JCPDS, No. 34-0394) and the internal standard Ni for sample x=0 to x=0.15, no other peak of impurities were detected. An amplification of the XRD patterns for sample $Ce_{1-x}Fe_xO_2$ shown in Fig. S1(II) indicated that there was an evident shift for CeO_2 (220) peak towards higher diffraction compared with that of pure CeO_2. This shift became more evident with the increment of x from 5% to 20%, and further increasing of Fe content to 25% didn't cause any significant shift compared with that of 20%.

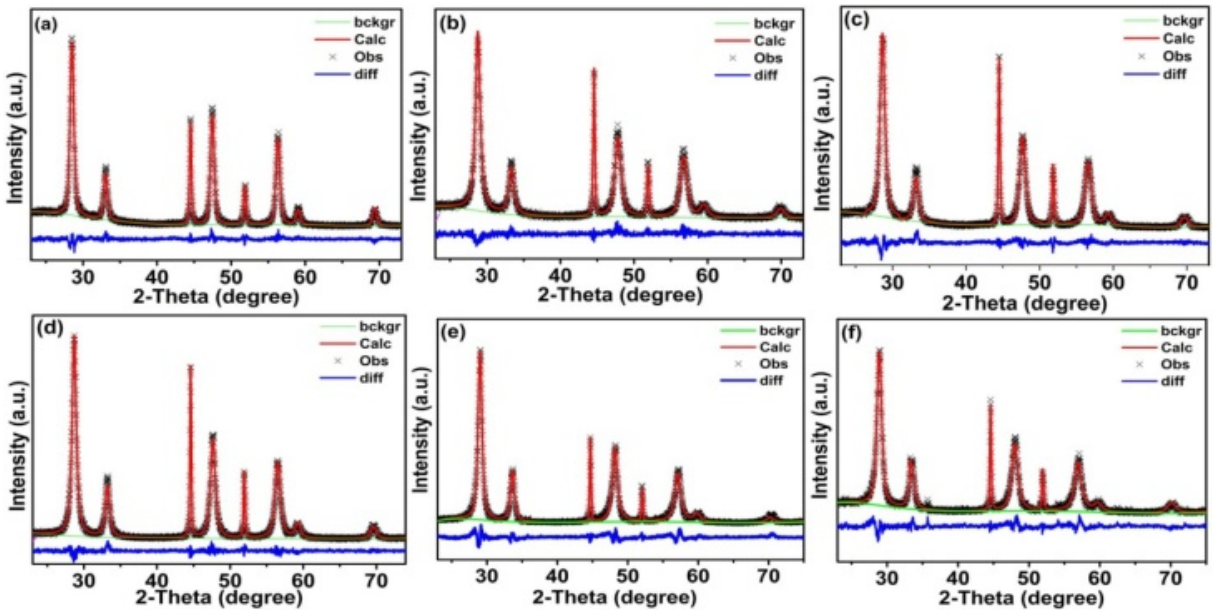

Fig. S2 Profile refined XRD patterns for $Ce_{1-x}Fe_xO_2$ systems at, (a) x=0, (b) x=0.05, (c) x=0.10, (d) x=0.15, (e) x=0.20, and (f) x=0.25.

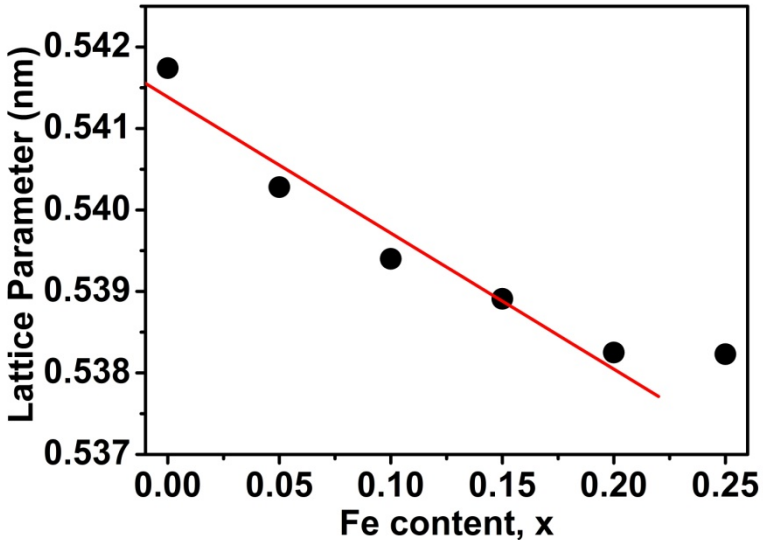

Fig. S3 Relationship between lattice parameter and Fe doping in $Ce_{1-x}Fe_xO_2$ (x=0~0.25).

As shown in Fig. S3, there exsits a linear relationship between lattice paremeter and Fe doping level in $Ce_{1-x}Fe_xO_2$ within the solution limit.

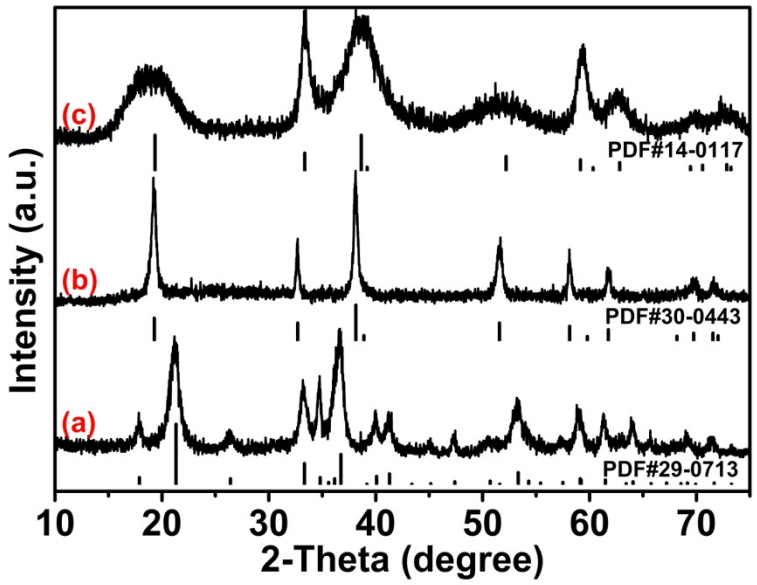

Fig. S4 XRD patterns of the intermediate product formed prior to the hydrothermal reactions of $Ce_{1-x}M_xO_2$-P (x=1) systems at (a) M=Fe, (b) M=Co, (c) M=Ni.

It could be observed from Fig. S4 that characteristics products for these three compounds were corresponding to α-FeOOH (JCPDS, No. 29-0713), $Co(OH)_2$ (JCPDS, No. 30-0443) and $Ni(OH)_2$ (JCPDS, No. 14-0117) for $Ce_{1-x}M_xO_2$-P (x=1) systems at M=Fe, Co, Ni, respectively.

Part 2. Relevant data and descriptions about synthesis mechanism of $Ce_{1-x}Fe_xO_2$ system

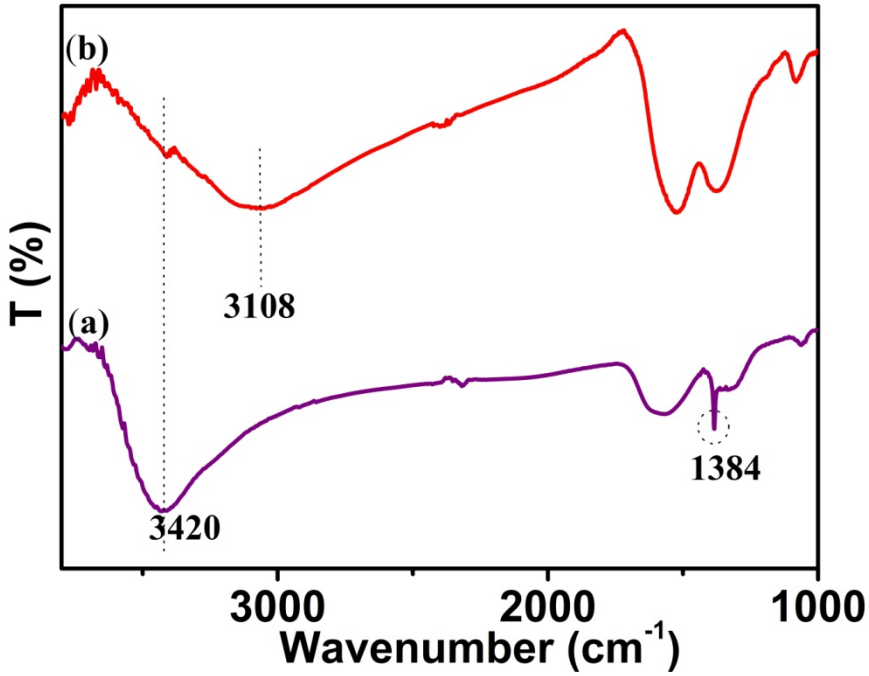

Fig. S5 IR spectra of (a) CeO_2-a and (b) $Ce_{0.9}Fe_{0.1}O_2$-a.

By characterization of flourier transform infrared (FTIR) spectra, an infrared band at 3420 cm^{-1} corresponding to hydroxyl groups from H_2O was observed for CeO_2 precursor after reacting at 220 ^oC for 1 min, no signal related to OH group of $Ce(OH)_4$ was observed. Its XRD patterns stayed the same with that of CeO_2-P (not given). All these phenomena indicate the transformation of $Ce(OH)_4$ to CeO_2, in accordance with what was reported before.[2] While for sample $Ce_{0.9}Fe_{0.1}O_2$ precursor, two signals at 3420 and 3108 cm^{-1} were both detected, which were from the absorbed H_2O species on CeO_2 and OH group of FeOOH, respectively. Besides, the infrared band at 1384 cm^{-1} corresponding to N-O stretching mode could only be detected for CeO_2 precursor, while not on that of $Ce_{0.9}Fe_{0.1}O_2$ precursor. It could be speculated that CeO_2 with FeOOH around was formed.

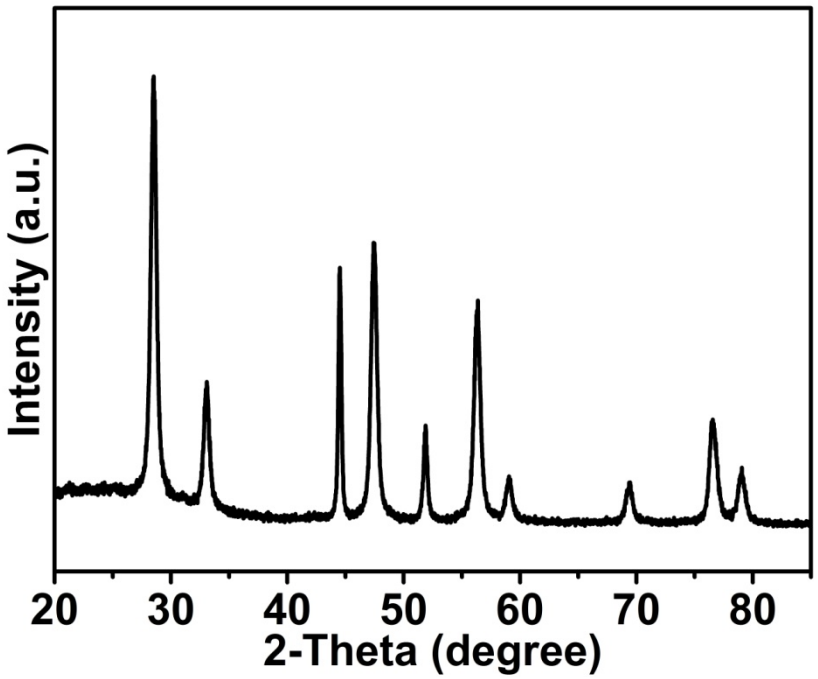

Fig. S6 XRD patterns of $Ce_{0.9}Fe_{0.1}O_2$-b.

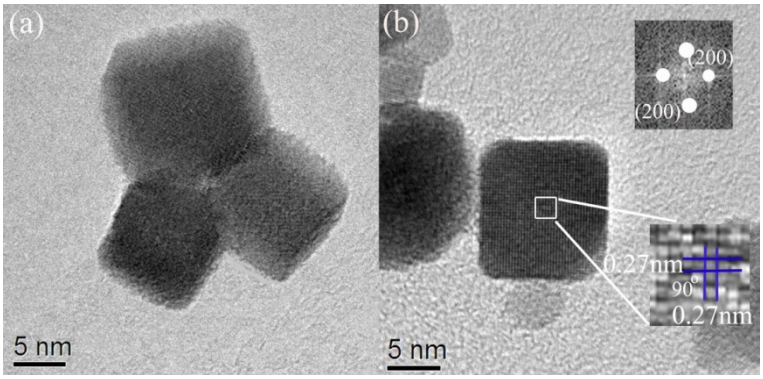

Fig. S7 HRTEM images of $Ce_{0.9}Fe_{0.1}O_2$. Inset of (b) is the high-resolved lattice fringes and the corresponding FFT result for the nanocube.

It could be observed from Fig. S6 (a) that three regular $Ce_{0.9}Fe_{0.1}O_2$ nanocubes were stacked together. Besides, the spacing of the fringes parallel to the top and bottom of the nanocube is 0.27 nm from the HRTEM images (Fig. S6 (b)), which is attributed to the (200) facet. In addition, the angle between (200) planes is 90 ^{o} on the basis of fast Fourier transform (FFT). Therefore, after 24 h hydrothermal treatment, $Ce_{0.9}Fe_{0.1}O_2$ nanocube with facet (200) exposed surface was synthesized.

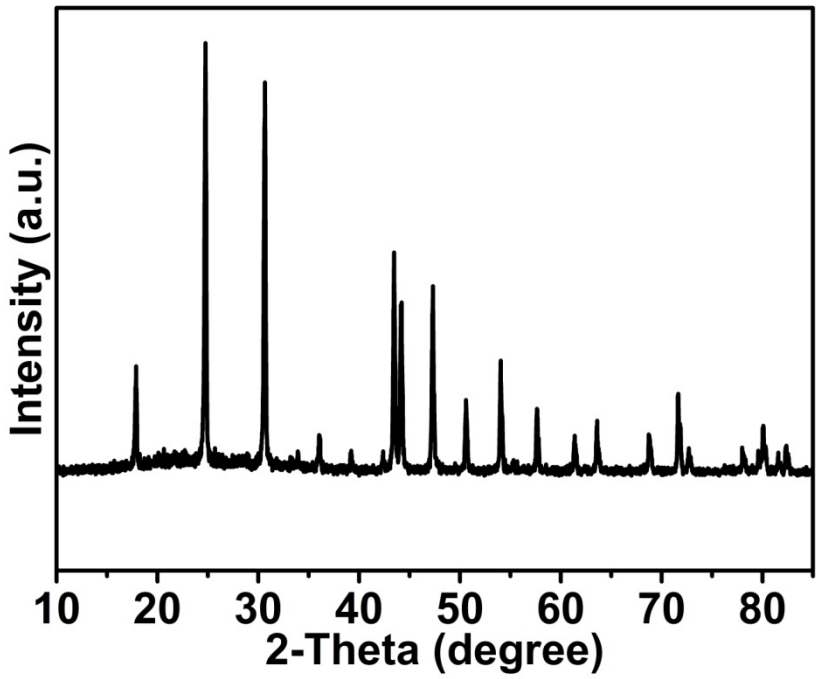

Fig. S8 XRD patterns of the sample Ce-Fe-U.

As observed from Fig. S5, all peaks could be assigned to $Ce(CO_3)(OH)$ (JCPDS, No. 52-0352) and no solid solutions are formed when urea is selected as the precipitant.

Part 3. Relevant data and descriptions about doping effect of Fe^{3+} on the structure

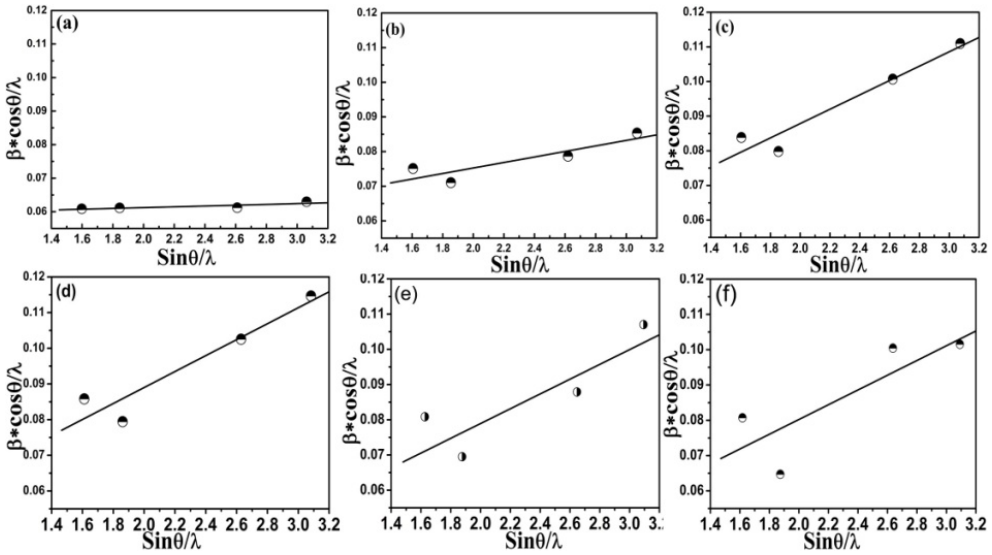

Fig. S9 Relationship between βcosθ/λ and sinθ/λ for $Ce_{1-x}Fe_xO_2$ at (a) x=0, (b) x=0.05, (c) x=0.10, (d) x=0.15, (e) x=0.20, and (f) x=0.25.

The mean lattice strain (η) and the mean crystallite size (D) could be calculated using the equation: $\beta\cos\theta/\lambda = 0.89/D + \eta\sin\theta/\lambda$, where β is the full width at half maximum (FWHM), θ is the diffraction angle, and λ is the X-ray wavelength.

Part 4. Relevant data and descriptions about doping effect of Fe^{3+} on catalytic performance

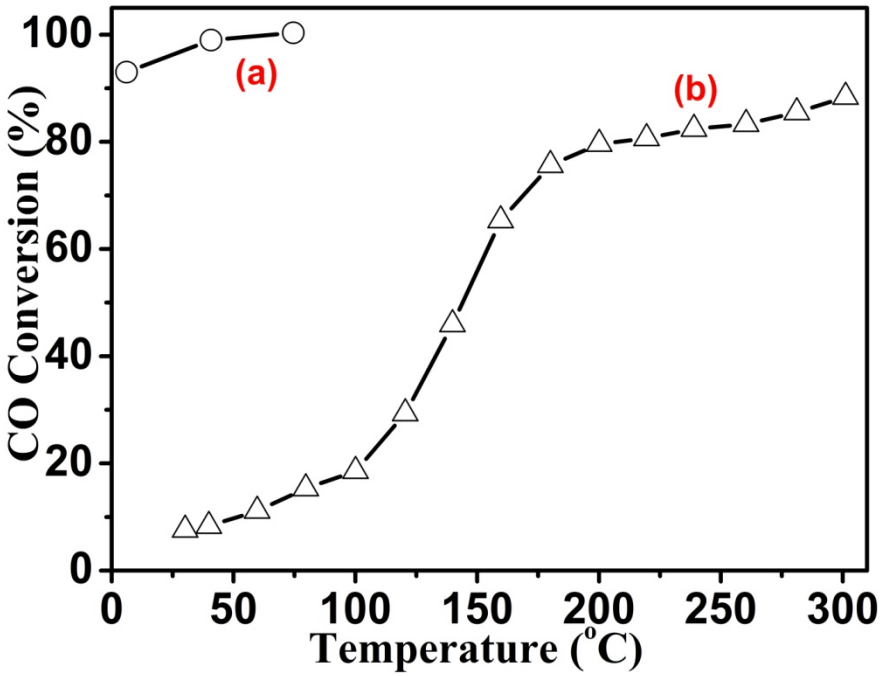

Fig. S10 Catalytic activity of supported Au catalysts redrawn from (a) Ref[3] and (b) Ref[4], respectively.

Notes and references

[1] Y. Zuo, X. Huang, L. Li and G. Li, *J. Mater. Chem. A*, 2013, 1, 374-380.

[2] C. S. Pan, D. S. Zhang, L. Y. Shi and J. H. Fang, *Eur. J. Inorg. Chem.*, 2008, 2429-2436.

[3] K. Qian, L. Luo, H. Bao, Q. Hua, Z. Jiang and W. Huang, *Catal. Sci. Technol.*, 2013, **3**, 679-687.

[4] R. Güttel, M. Paul and F. Schüth, *Catal. Sci. Technol.*, 2011, **1**, 65-68.